

KINEMATIC ANALYSIS OF PLANAR CABLE-DRIVEN ROBOTS WITH PARALLELOGRAM LINKS

N. Khodadadi¹, M. Isaac Hosseini¹, S. A. Khalilpour¹, H. D. Taghirad¹, Philippe Cardou²

¹*Advanced Robotics and Automated Systems (ARAS), Faculty of Electrical Engineering*

K. N. Toosi University of Technology, Tehran, Iran.

²*Department of Mechanical Engineering, Robotics Laboratory, Laval University, Quebec City, Canada.*

*Email: khodadadi, mohammadisaac.hosseini@email., khalilpour@ee., taghirad@kntu.ac.ir
and pcardou@gmc.ulaval.ca*

ABSTRACT

Employing redundant cables to control the moving platform of cable-driven parallel robots (CDPRs) not only ensures that the cables are in tension during the robot maneuvers, but can also significantly improve the kinematic performance indices of the robot. This paper presents a new structure for planar CDPRs that use parallelogram links instead of conventional links, to preserve both of these characteristics. Exploiting parallelogram links eliminates the necessity to use additional actuators in the design of planar CDPRs, while redundancy of cables is still preserved in the robot structure. The main innovation of the paper is to provide a general formulation for the proposed structure that covers all possible designs for planar CDPRs, such that the most suitable design is adopted for the demanded application. The proposed structure is applied to two cases of planar CDPRs, namely fully constrained and redundantly actuated, while the simulation results verifies the effectiveness of the proposed analysis.

Keywords: kinematic analysis, cable-driven parallel manipulator, parallel mechanism, parallelogram structure.

L'ANALYSE CINÉMATIQUE DES ROBOTS PARALLÈLES ENTRAÎNÉS PAR CÂBLES AVEC DES MEMBRES EN PARALLÉLOGRAMMES

RÉSUMÉ

L'utilisation de câbles redondants pour le contrôle de l'effecteur dans les robots parallèles entraînés par câbles (RPEC) permet non seulement d'assurer que les câbles demeurent en tension, mais améliore aussi les indices de performance cinématique du robot. Cet article présente une nouvelle structure de RPEC plan qui inclut des membres en parallélogrammes pour préserver ces deux avantages. En exploitant les membres en parallélogrammes, on s'affranchit du besoin d'avoir des actionneurs redondants dans le RPEC tout en maintenant un nombre de câbles supérieur au minimum nécessaire. L'innovation principale de cet article consiste à fournir un modèle mathématique assez général pour représenter tous les concepts possibles de RPEC plans avec parallélogrammes, permettant d'analyser une grande variété de concepts et de retenir celui qui est le mieux adapté à une application donnée. En guise d'exemple, la formulation proposée est appliquée à deux RPEC plans : l'un qui possède un actionnement minimal et l'autre, un actionnement redondant. Les résultats des analyses semblent corroborer l'utilité de la méthode proposée.

Mots-clés : analyse cinématique; robot parallèle entraîné par câbles; mécanisme parallèle; membre en parallélogramme.

1. INTRODUCTION

A cable-driven parallel robot (CDPR) consists of a fixed frame, the actuators, the cables and guiding pulleys, and a moving platform. Each cable connects the moving platform to the actuators via one or several guide pulleys. By this means, actuators manipulate the moving platform toward the desired position and orientation by controlling the length of the cables [1]. Large workspace, fast motion, ease of construction are only some of the unique features attributed to the CDPRs. Thanks to these advantages, CDPRs have been used in various practical applications such as large radio telescopes, rescue missions in dangerous environments, medical rehabilitation equipment and video capturing [2].

Despite all of these brilliant features of cable robots, this class of robots suffers from being capable to exert only tensile force in the cables, and having usually low stiffness. However, if actuator redundancy is considered in the design of CDPRs, the kinematic performance indices such as stiffness, dexterity, and workspace of the robot are upgraded, while it will ensure that the cables remain in tension during all robot maneuvers [3].

A n degree-of-freedom robot driven by m actuators may be classified into three general categories [4, 5]:

- Under-actuated ($n > m$): In this category of CDPRs, not all n degrees of freedom can be simultaneously controlled by the m actuators, and the cable tensions derive uniquely from a passive external force such as gravity [6].
- Suspended Fully-constrained ($n = m$): In this category of CDPRs, all degrees of freedom are controlled by the actuators, while the cable tensions are also derived uniquely from the platform weight or other passive external forces [7].
- Over-constrained ($n < m$): In this category of CDPRs, all degrees of freedom are controlled by the actuators, and there is a $(m - n)$ -dimensional set of cable tensions that allow the robot to remain in equilibrium, $m - n$ being the number of extra actuators. The cables remain in tension either by working in opposition to one another [8] or by a passive force such as weight [9, 10].

Adding actuator redundancy in the robot structure, increases its cost and the challenge posed by its control. For this purpose, given the importance of redundancy and its challenges, this paper presents a new structure for cable robots that eliminates the need for additional actuators while redundancy of cables is still preserved in the robot structure. In the proposed structure, parallelogram links are used instead of conventional links, such that each parallelogram link of the robot consists of one or two independent cables, and each cable is directly controlled by an actuator. Therefore, there are always more cables than actuators in the proposed structure. According to how the links are controlled by the actuators, different designs may be considered for the proposed structure.

The idea of using parallelogram in CDPRs has been previously used in 3D spatial cable robots [11, 12]. Despite the overall positive feature of this novel structure, very few CDPRs are based on this idea. Furthermore, to the best of the authors' knowledge, planar CDPRs robots with parallelogram links have not been reported in the literature. Therefore, the main contribution of this paper is to present different designs with parallelogram structure for planar CDPRs and to analyse their kinematic performance. The main goal of this paper is to show how we can use the benefits of redundant cables in the robot's geometry without the cost of extra actuators. Accordingly, a kinematic formulation that covers all possible designs for planar CDPRs (either with the proposed structure or with a traditional structure) is presented in this paper. The designer can use this formulation to adopt the most suitable design according to the application at hand. Furthermore, the efficiency of the proposed structure is evaluated by its applying it to two cases of planar CDPRs, and the results are compared with the traditional structures. The simulation results illustrate that, compared to traditional structures, kinematic performance indices have been significantly increased.

The paper is organized as follows. Section II describes the proposed structure elaboration with a few illustrative examples. Section III is dedicated to kinematic modeling of the proposed structure and presentation of a general formulation to it. Section IV introduces the kinematic performance indices that express the workspace, dexterity, and stiffness of the robot. Simulation results and comparisons are presented in section V. Finally, the concluding remarks are given in Section VI. Note that in all analysis, the cables are assumed to have negligible mass, so that any sagging effect is neglected. This assumption holds for CDPRs that do not have a relatively large workspace [13].

2. STRUCTURE DESCRIPTION

Contrary to the traditional structures of cable robots, in which each robot link consists of only one single cable, in the proposed structure, the robot links are made of parallelogram cables. Let us first consider the three cable designs illustrated in Fig. 1. In the first design, the cable from the actuator is directly connected to the moving platform. This design is not capable of reduce the lateral movements and vibrations. In other words, the stiffness of the robot is low in the horizontal direction. Instead of using a single cable, in the second design, the cable is connected to a fixed point on the base frame by installing a pulley on the moving platform. Since in this design, the moving platform is pulled by a pair of cables, the robot has more load-carrying capacity while its undesirable oscillations may be reduced. In the third design, similar to the second one, a pulley is installed on the moving platform, with the difference that the angles of cable entry and exit to the pulley are not the same, and is a function of the position of the moving platform. Therefore, in this design, both undesirable vibrations and lateral displacements may be greatly attenuated.

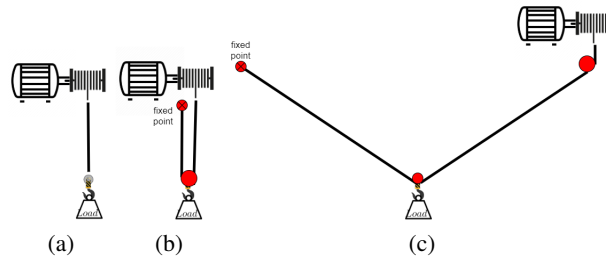


Fig. 1. Three simple designs of suspended 1DOF cable robot. (a) Simple design that cable directly connected to end-effector. (b) and (c) Using couple of cables design.

In order to describe the proposed structure, a general planar CDPR based on this structure is presented in Fig. 2. The proposed structure is not limited to planar CDPRs and may be generalized to 3D cable robots [11, 12], but for the sake of simplicity, the concept of the proposed structure on a planar model is analyzed here. As shown in Fig. 2, the proposed structure uses parallelogram links, which may consist of one or two independent cables, instead of using conventional links that include only a single cable. In this figure, A_j and B_j represent the anchor points located on the base frame and the moving platform of the robot, respectively, each of which may be either a fixed point or a guiding pulley. Furthermore, denote k and m as the number of cables that pull the moving platform, and the number of actuators, respectively.

3. KINETOSTATIC ANALYSIS

In this section, a general formulation for kinetostatic analysis of the planar CDPRs with parallelogram cables is given. As shown in Fig. 2, two coordinate systems are defined. One is the fixed reference frame with origin O located on the lower-corner of the figure; the other is the moving reference frame that is

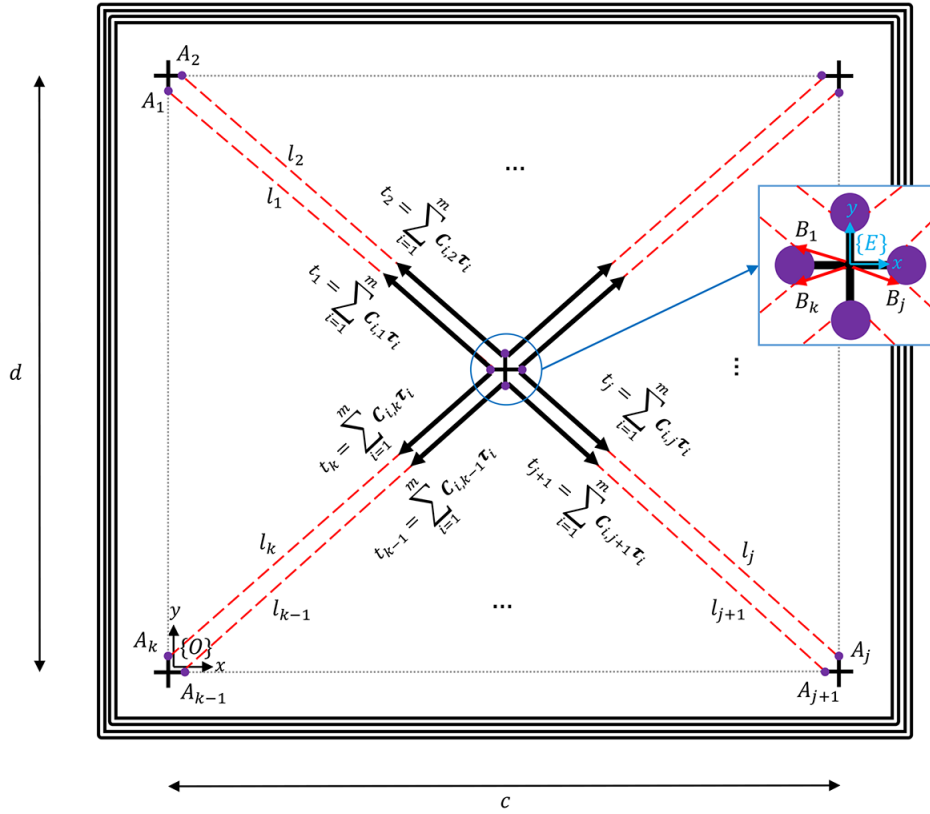


Fig. 2. A general planar CDPR with parallelogram links.

attached to the moving platform with its origin denoted by E . The vector \mathbf{l}_j from B_j to A_j is given by

$$\mathbf{l}_j = \mathbf{a}_j - \mathbf{p} - \mathbf{R}\mathbf{b}_j, \quad (1)$$

in which \mathbf{a}_j denotes the location of the anchor point A_j and \mathbf{p} is the position of the moving platform center, both with respect to fixed coordinate. \mathbf{b}_j is the position of the anchor point B_j in the moving coordinate system, and \mathbf{R} is the rotation matrix corresponding to a change of coordinates from the moving frame to the fixed frame. Let us define the direction of the j^{th} cable by the unit vector:

$$\mathbf{u}_j = \frac{\mathbf{l}_j}{\|\mathbf{l}_j\|}, \quad (2)$$

in which, $\|\mathbf{l}_j\|$ denotes the length of the j^{th} cable. According to the above definition, the static force and moment equilibrium of the CDPR may be represented by [14]:

$$\mathbf{U}\mathbf{t} = -\mathbf{w}_p, \quad (3)$$

where \mathbf{w}_p is the external wrench applied to the moving platform, while $\mathbf{t} = [t_1 \ t_2 \ \dots \ t_k]^T$ denotes the vector of cable forces. The \mathbf{U} matrix in the above equation may be calculated as follows [15]:

$$\mathbf{U} = \begin{bmatrix} \mathbf{u}_1 & \dots & \mathbf{u}_j & \dots & \mathbf{u}_k \\ \mathbf{R}\mathbf{b}_1 \times \mathbf{u}_1 & \dots & \mathbf{R}\mathbf{b}_j \times \mathbf{u}_j & \dots & \mathbf{R}\mathbf{b}_k \times \mathbf{u}_k \end{bmatrix}. \quad (4)$$

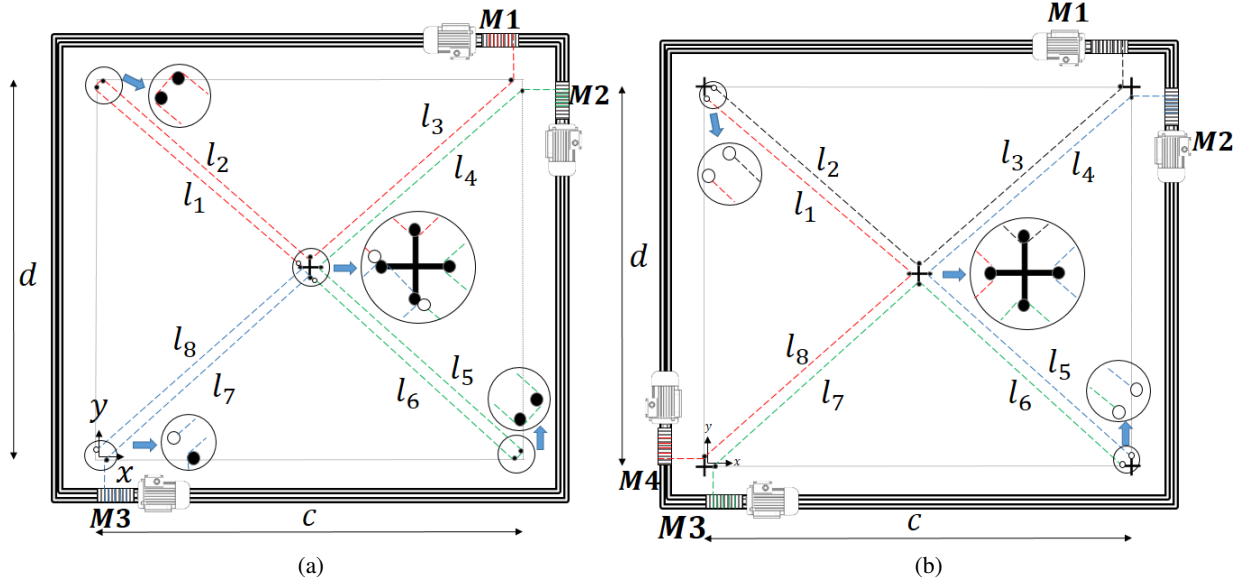


Fig. 3. Schematic diagram of two planar CDPR with parallelogram cables (a) with 3 actuators, (b) with 4 actuators. The filled circles show the pulleys and the empty circles demonstrate the fixed anchor points

Now, let us derive the relation between actuator forces and cable forces. Since a parallelogram structure is used in here, and the cables do not directly connect the moving platform to the actuators, the j^{th} cable tension is not equal to j^{th} actuator force. With the assumption that guiding pulleys have no friction, the tension remains constant along all cables. The relationship between the actuator forces and the cable tensions can thus be mathematically modeled by the linear mapping:

$$\mathbf{t} = \mathbf{C}^T \boldsymbol{\tau}, \quad (5)$$

in which \mathbf{C} is the $m \times k$ transmission matrix and \mathbf{t} denotes the vector of cable forces with k elements. Furthermore, $\boldsymbol{\tau}$ denotes the vector of actuator forces consisting of m elements. Therefore, the elements of \mathbf{C} may be defined as $c_{i,j}$ in which $i = 1, \dots, m$ and $j = 1, \dots, k$. The value of $c_{i,j}$ is equal to one when the j^{th} cable is connected to the i^{th} actuator either directly or via some guiding pulleys. Otherwise, $c_{i,j}$ is equal to zero. For example, in traditional structures, in which all cables directly connect the actuator to the moving platform and there is no parallelogram of cables, the \mathbf{C} matrix is given by $\mathbf{C} = \mathbf{I}_{m \times m}$. Other CDPRs with parallelogram links such as those seen in Fig. 3 require a different definition of \mathbf{C} , however. In the first design, which is shown in Fig. 3a, three actuators are used to manipulate the moving platform in the xy plane. As it is seen in this figure, in this design the first actuator controls the first three cable forces, namely, t_1 , t_2 , and t_3 , the second actuator controls t_4 , t_5 and t_6 , and the third actuator controls t_7 and t_8 . Hence, the transmission matrix \mathbf{C} for this design is as follows

$$\mathbf{C} = \begin{bmatrix} 1 & 1 & 1 & 0 & 0 & 0 & 0 & 0 \\ 0 & 0 & 0 & 1 & 1 & 1 & 0 & 0 \\ 0 & 0 & 0 & 0 & 0 & 0 & 1 & 1 \end{bmatrix}, \quad (6)$$

The schematic diagram of the second proposed scheme is shown in Fig. 3b. In this design, four actuators have been used to control the two degrees of freedom of a point on the $x - y$ plane. As the schematic diagram of this structure shows, the cables l_2 and l_3 are connected to one another through a guiding pulley. Similarly,

the relation between other cable forces with respect to the actuators may be expressed as:

$$\mathbf{C} = \begin{bmatrix} 0 & 1 & 1 & 0 & 0 & 0 & 0 & 0 \\ 0 & 0 & 0 & 1 & 1 & 0 & 0 & 0 \\ 0 & 0 & 0 & 0 & 0 & 1 & 1 & 0 \\ 1 & 0 & 0 & 0 & 0 & 0 & 0 & 1 \end{bmatrix}. \quad (7)$$

To further continue the kinetostatic analysis, substitute Eq. (5) into Eq. (3), to rewrite the static force equilibrium as:

$$\underbrace{\mathbf{UC}^T}_{\mathbf{A}} \boldsymbol{\tau} = -\mathbf{w}_p, \quad (8)$$

where $\mathbf{A} = \mathbf{UC}^T$ is known as the wrench or structural matrix of the robot. This matrix is the transpose of the Jacobian matrix mapping actuator's velocities onto the moving platform velocity:

$$\mathbf{J} = -\mathbf{A}^T. \quad (9)$$

It should be noted that the overall length of a cable connecting an actuator through some guiding pulleys to a fixed point, may be calculated as

$$\mathbf{l}_T = \mathbf{C}\mathbf{l}, \quad (10)$$

where \mathbf{l}_T is the unstretched cable length, $\mathbf{l} = [l_1, l_2, \dots, l_k]^T$, and $l_j = \|\mathbf{l}_j\|$ is the length of j^{th} cable.

4. KINEMATIC PERFORMANCE INDICES

4.1. Dexterity Index

The dexterity index of a robot is introduced through the condition number of the Jacobian matrix. Since the Jacobian depends on the pose of the moving platform in the workspace, the value of its condition number indicates how close the robot is to singularity. This index ranges from one (isotropy) to infinity (singularity) and, when it is based on the 2-norm of the matrix, it can be computed as [16]:

$$\kappa_{\mathbf{J}} = \frac{\sigma_{max}}{\sigma_{min}}, \quad (11)$$

where σ_{max} and σ_{min} are the maximum and minimum singular values of the Jacobian matrix, respectively. In order to make a clear comparison between the robot structures, we use the inverse of the dexterity index, $\kappa_{\mathbf{J}}^{-1}$, which is normalized in the interval $[0, 1]$. These indices describe only the local performance of a robot at a specific configuration. Therefore, in order to measure the global dexterity of a robot, one may use a global dexterity index (GDI) [17], such as:

$$GDI = \frac{\int_W \kappa_{\mathbf{J}}^{-1} dW}{\int_W dW}, \quad (12)$$

in which W denotes the volume of the robot's workspace.

4.2. Stiffness Index and Stiffness Magnitude

The passive stiffness of a CDPR depends solely on the cables elasticity and the configuration of the moving platform, and may be obtained as follows [18]:

$$\mathbf{K}_p = \mathbf{J}^T \boldsymbol{\Omega} \mathbf{J}, \quad (13)$$

in which

$$\mathbf{\Omega} = \text{diag}(k_1, \dots, k_m), \quad k_i = \frac{E_i S_i}{l_{T_i}}, \quad (14)$$

where E_i and S_i represent Young's modulus of elasticity, and the cross-section area of the i th cable, respectively, while, l_{T_i} is defined in Eq. (10). Accordingly in [19], the 2-norm condition number of the passive stiffness matrix is introduced as the stiffness index for CDPRs. This index, like the dexterity index, ranges from one to infinity, and can be written as

$$\kappa_{\mathbf{K}_p} = \frac{\lambda_{max}}{\lambda_{min}}, \quad (15)$$

where λ_{max} and λ_{min} are the largest and smallest eigenvalues of the passive stiffness matrix, respectively. It is clear that the desired value of this index is equal to 1, and values greater than 1 ($\kappa_{\mathbf{K}_p} \gg 1$) indicate a lack of uniform distribution of stiffness along all degree of freedoms (DOF). As before, the inverse of this index $\kappa_{\mathbf{K}_p}^{-1}$ is used instead here, which ranges from zero to one, and a global stiffness index (GSI) may be given by:

$$GSI = \frac{\int_W \kappa_{\mathbf{K}_p}^{-1} dW}{\int_W dW}. \quad (16)$$

To measure the stiffness magnitude, Yeo et al. have also suggested the following index [20]:

$$M = \frac{\lambda_{max}^2 \lambda_{min}^2}{\lambda_{max}^2 + \lambda_{min}^2}. \quad (17)$$

One of the design goals is definitely to have the maximum possible stiffness magnitude for the robot, which according to Eq. 17 is achievable when λ_{max} , λ_{min} are equal and are sufficiently large. Similarly, a global index for the stiffness magnitude may be derived as $GSM = (\int_W M dW) / (\int_W dW)$.

4.3. Wrench Closure Workspace

The controllable workspace or wrench closure workspace (WCW) is the set of poses for which any arbitrary wrench w_p applied to the end-effector can be balanced by positive cable tensions, i.e., for which there is a solution to the constraint satisfaction problem $\mathbf{A}\boldsymbol{\tau} = -\mathbf{w}_p$ and $\boldsymbol{\tau} \geq \mathbf{0}_m$. One of the most important theorems about the analysis of this kind of workspace is based on computing the null space of the wrench matrix. Based on the features of the null space, position of the end-effector belongs to controllable workspace, if and only if, the wrench matrix of the manipulator is of full rank and linear combination of its null space vectors contains a vector whose elements have all the same sign [21].

In this paper, we wish to consider the WCW in the optimal design of CDPRs. To this end, the workspace is sampled with a grid of moving-platform poses, and we retain those that can be reached with the moving platform. Next the linear combination of null space vectors of the wrench matrix is calculated for all reachable poses and if a positive linear combination of null space vectors is feasible then the pose belongs to the WCW [21]. In order to have a global index related to the size of the area of WCW, the ratio of number of wrench-closure poses to the total number of poses of the grid may be used.

5. SIMULATION AND DISCUSSION

This section is dedicated to the kinematic analysis of the two CDPR designs illustrated in Fig. 3. As previously stated, due to the parallelogram structure, both designs are fully-constrained and have better kinematic performance than traditional ones. To show this, we make several comparisons with respect to the indices introduced in the last section and show how parallelogram cables can be used to improve the robot's performance.

5.1. Over-constrained Planar CDPR With Three Actuators

5.1.1. Parallelogram Design

In this section, based on the coefficient matrices calculated in the previous section, we aim to derive the kinematic equations for the robot shown in Fig. 3a. According to Eqs. (6) and (8), the wrench matrix may be obtained as

$$\mathbf{A} = - \begin{bmatrix} \frac{x}{l_1} + \frac{x}{l_2} + \frac{(x-c)}{l_3} & \frac{(y-d)}{l_1} + \frac{(y-d)}{l_2} + \frac{(y-d)}{l_3} \\ \frac{(x-c)}{l_4} + \frac{(x-c)}{l_5} + \frac{(x-c)}{l_6} & \frac{(y-d)}{l_4} + \frac{y}{l_5} + \frac{y}{l_6} \\ \frac{x}{l_7} + \frac{x}{l_8} & \frac{y}{l_7} + \frac{y}{l_8} \end{bmatrix}^T_{3 \times 2} \quad (18)$$

in which

$$\begin{aligned} l_1 = l_2 &= \sqrt{x^2 + (y-d)^2}, l_3 = l_4 = \sqrt{(x-c)^2 + (y-d)^2}, \\ l_5 = l_6 &= \sqrt{(x-c)^2 + y^2}, l_7 = l_8 = \sqrt{x^2 + y^2}, \end{aligned} \quad (19)$$

and $c = d = 1$ m denote the width and height of the robot fixed attachment points, respectively. According to Eq. (10), the overall cable length may also be derived as:

$$l_{T_1} = l_1 + l_2 + l_3, \quad l_{T_2} = l_4 + l_5 + l_6, \quad l_{T_3} = l_7 + l_8, \quad (20)$$

where, $l_{T_i}, i = 1 \cdots, 3$ are the elements of the vector \mathbf{l}_T defined in Eq. (10).

5.1.2. Traditional Design

Figure 4a shows the simplest and traditional design of fully-constrained planar CDPRs. As is shown in this figure, this robot has a triangular structure and its moving platform is controlled by three links, each of which is directly and independently connected to an actuator. The transmission matrix in this design, like all traditional designs of CDPRs, is an identity matrix, $\mathbf{C} = \mathbf{I}_{m \times m}$, where $m = 3$ represents the number of actuators. Therefore, the wrench matrix \mathbf{A} may be easily determined as

$$\mathbf{A} = - \begin{bmatrix} \frac{x}{l_1} & \frac{(x-c)}{l_2} & \frac{(x-c/2)}{l_3} \\ \frac{(y-d)}{l_1} & \frac{(y-d)}{l_2} & \frac{y}{l_3} \end{bmatrix}_{2 \times 3}. \quad (21)$$

5.1.3. Analysis and Discussion

The kinematic performance indices of both designs are shown in Fig. 5. The dashed line in Figs. 5a and 5d shows the boundary of the wrench-closure workspace. As it can be seen from these figures, the area of the WCW in the proposed design with parallelogram cables has been significantly increased. It may be reported that WCW in the triangular structure covers a maximum of 50% of the total workspace of the robot, while this index for the proposed structure is increased to 66%. The dexterity index of the robots are also displayed in Figs. 5a and 5d. As shown in these figures, most of the workspace for the proposed structure has a dexterity index larger than 0.7 indicating the effectiveness of this structure for fully-constrained planar CDPRs. The area with such dexterity measure the traditional design is much smaller and located only at the center of the triangular workspace. Figures 5b to 5f show the stiffness index and its magnitude. As expected, the use of parallelogram links in the proposed structure has not only been able to improve the stiffness index but has also greatly expanded the desired areas in terms of this index. Furthermore, the stiffness magnitude index of the traditional design in the best position of the moving platform is equal to 2.7, while much higher values can be obtained in most of the workspace of the proposed design.

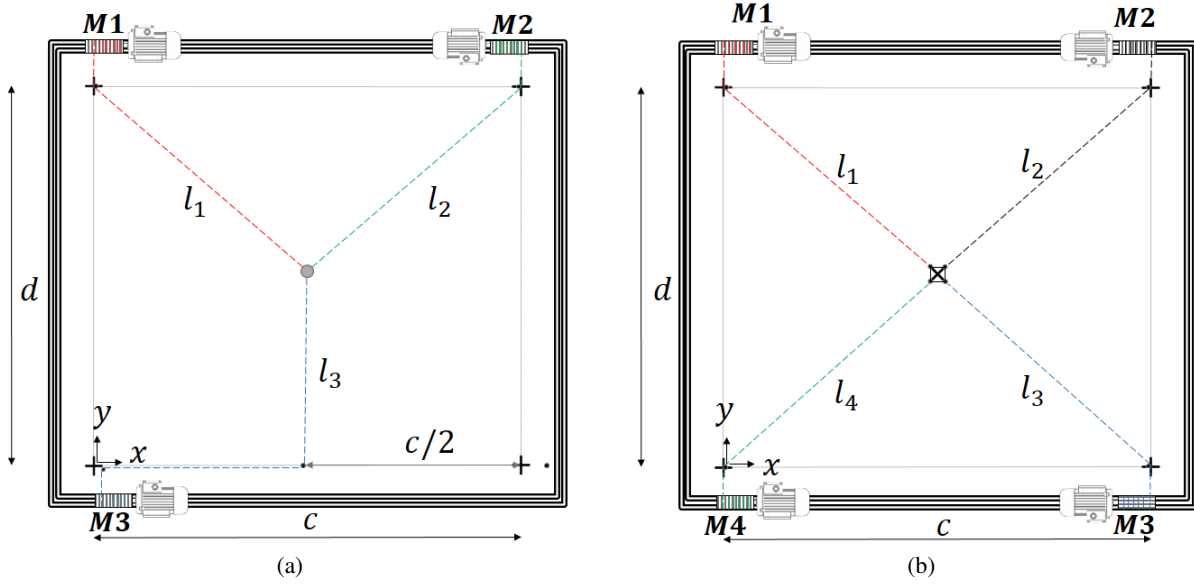


Fig. 4. Schematic diagram of traditional designs: (a) an over-constrained CDPR with two DoF and three motors (b) an over-constrained CDPR with two DoF and four motors.

5.2. Over-constrained Planar CDPR With Four Actuators

In this section, Let us add an extra actuator to both of the traditional and parallelogram designs to investigate the kinematic performance in redundant situations. The schematic diagrams of the redundant CDPR with parallelogram links and the traditional one are shown in Figs. 3b and 4b, respectively.

5.2.1. Parallelogram Design

According to the coefficient matrix obtained in Eq. (7), the wrench matrix may be determined by:

$$\mathbf{A} = - \begin{bmatrix} \frac{x}{l_2} + \frac{(x-c)}{l_3} & \frac{(y-d)}{l_2} + \frac{(y-d)}{l_3} \\ \frac{(x-c)}{l_4} + \frac{(x-c)}{l_5} & \frac{(y-d)}{l_4} + \frac{y}{l_5} \\ \frac{(x-c)}{l_6} + \frac{x}{l_7} & \frac{y}{l_6} + \frac{y}{l_7} \\ \frac{x}{l_1} + \frac{x}{l_8} & \frac{(y-d)}{l_1} + \frac{y}{l_8} \end{bmatrix}_{4 \times 2}^T. \quad (22)$$

Based on Eq. (10), the overall length of cables may also be obtained as:

$$l_{T1} = l_2 + l_3, \quad l_{T2} = l_4 + l_5, \quad l_{T3} = l_6 + l_7, \quad l_{T4} = l_1 + l_8, \quad (23)$$

where parameters $l_j, j = 1, \dots, 8$ and $l_{T_i}, i = 1, \dots, 4$ are the elements of the vectors \mathbf{l}, \mathbf{l}_T , respectively, as defined in Eq. (10).

5.2.2. Traditional Design

The traditional design of the redundant fully-constrained planar CDPRs, like the proposed structure, has a square wrench-closure workspace. The schematic diagram of this design is shown in Fig. 4b. As before, the transmission matrix in this design is equal to the identity matrix ($\mathbf{C} = \mathbf{I}_{m \times m}$ where $m = 4$). Thus, according to Eq. (8), the wrench matrix can be calculated as follows

$$\mathbf{A} = - \begin{bmatrix} \frac{x}{l_1} & \frac{(x-c)}{l_2} & \frac{(x-c)}{l_3} & \frac{x}{l_4} \\ \frac{(y-d)}{l_1} & \frac{(y-d)}{l_2} & \frac{y}{l_3} & \frac{y}{l_4} \end{bmatrix}_{2 \times 4}. \quad (24)$$

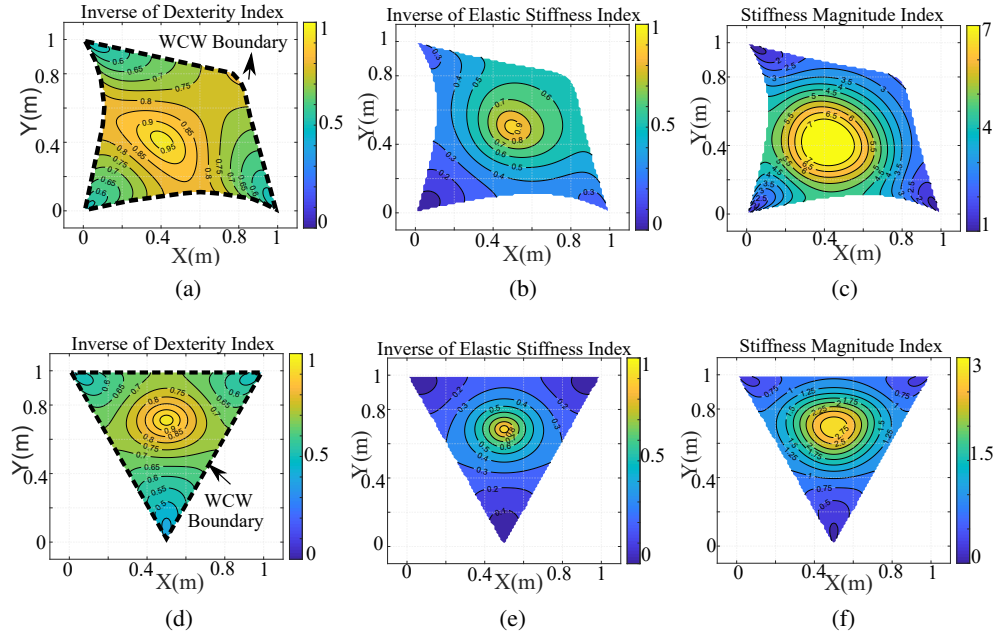


Fig. 5. Kinematic performance indices of two 2-DoF over-constrained planar cable-driven parallel robots driven by three motors. The graphs in the first row correspond to the parallelogram design shown in Fig. 3a, while those in the second row correspond to the traditional design shown in Fig. 4a. (a), (d) Inverse of dexterity index, (b), (e) inverse of stiffness index, (c), (f) normalized stiffness magnitude index of proposed and traditional design, respectively.

5.2.3. Analysis and Discussion

Since four actuators are used for 2 DOF in both designs, it is expected that the kinematic performance indices would be significantly improved. Figs. 6 show that compared to the fully-constrained planar CDPRs analysed in the last section, the proposed designs have larger workspace and better kinematic performances. As demonstrated in Figs. 6a and 6d, the WCW of both designs covers 100% of the workspace of the robot. The dexterity index, also shown in these figures, has also increased significantly for both robots. However, the proposed design has been able to provide larger workspace with better dexterity when compared to that of the traditional design. In order to analyze the stiffness of both robots, the stiffness index and its magnitude are illustrated in Figs. 6b to 6f, where the proposed structure clearly demonstrates its effectiveness. Very suitable stiffness index are obtained in most configurations within the workspace of the proposed design, while for the traditional design this is limited to the center of the workspace. On the other hand, although the maximum stiffness magnitude for the proposed design is a bit smaller than that of the traditional design, its average stiffness over the workspace appears higher. It can be seen that in the traditional design, the stiffness magnitude index drops sharply when the robot is moving away from the center of the workspace.

Finally, for the sake of quantitative comparisons for all of the designs, global kinematic performance indices are given in Table 1. The results of this table clearly show that parallelogram cables in the robot structure can increase its performance indices. For instance, the GDI value in the three-motor category has been increased from 0.68 to 0.76. On the other hand, this enhancement for the GSM index is about 3.43. In the four-motor, although the values of the performance indices are closer to each other, (and in one such case, the WCW indices are equal) the proposed structure shows its superiority over the traditional structure in indices such as GSI and GSM, which have increased by the factors 1.84 and 1.10, respectively. In addition, some indices such as the GSI and GSM in the proposed design with three motors, are even better than the traditional design with four motors.

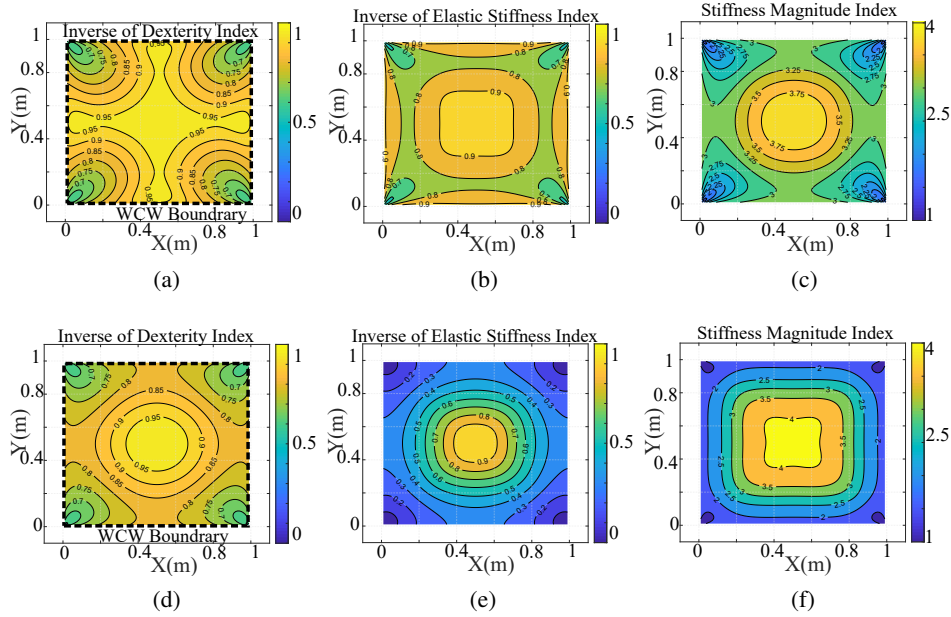


Fig. 6. Kinematic performance indices of the two 2-DoF over-constrained planar cable-driven parallel robots driven by four motors. The graphs in the first row correspond to the proposed parallelogram design shown in Fig. 3b, while those in the second row correspond to the traditional design shown in Fig. 4b. (a), (d) Inverse of dexterity index, (b), (e) inverse of stiffness index, (c), (f) normalized stiffness magnitude index of proposed and traditional design, respectively.

6. CONCLUSIONS

In this paper, a new structure for planar cable-driven parallel robots is proposed, in which parallelogram links are used instead of conventional links. In this structure, unlike the traditional structure, each link is not necessarily controlled by only one actuator. A general formulation for such structure was introduced in this paper, which can be used for all possible designs of planar CDPRs. This formulation helps the designer to select the best design for his or her robot in terms of different dexterity measures. Furthermore, different kinematic and dexterity measures are reviewed in this paper, and are used to compare the proposed structural design of parallelogram links to their conventional counterparts. In the reported results, it is observed that the proposed structures based on parallelogram links could significantly improve the wrench-closure workspace, while greatly and widely improving kinematic performance indices such as the dexterity and the stiffness of the robot.

REFERENCES

1. Hosseini, M.I., Harandi, M.J., Khalilpour, S.A. and Taghirad, H.D. "Experimental performance of adaptive fast terminal sliding mode control on a suspended cable robot." *Journal of Electrical and Computer Engineering Innovations (JECEI)*, Vol. 7, No. 1, pp. 59–67, 2019.
2. Gosselin, C. "Cable-driven parallel mechanisms: state of the art and perspectives." *Mechanical Engineering Reviews*, Vol. 1, No. 1, pp. DSM0004–DSM0004, 2014.
3. Jamshidifar, H., Khosravani, S., Fidan, B. and Khajepour, A. "Vibration decoupled modeling and robust control of redundant cable-driven parallel robots." *IEEE/ASME Transactions on Mechatronics*, Vol. 23, No. 2, pp. 690–701, 2018.
4. Khalilpour, S., Loloie, A.Z., Masouleh, M.T. and Taghirad, H. "Kinematic performance indices analyzed on four planar cable robots via interval analysis." In "2013 First RSI/ISM International Conference on Robotics

Category	Design	GDI	GSI	GSM	WCW
Fully-constrained	Proposed	0.76	0.47	4.50	0.66
	Traditional	0.68	0.31	1.31	0.50
Redundant	Proposed	0.87	0.83	3.10	1.00
	Traditional	0.82	0.45	2.80	1.00

Table 1. Kinematic performance indices

- and Mechatronics (ICRoM),” pp. 313–318. IEEE, 2013.
5. Khalilpour, S.A., Taghirad, H.R., Tale Masouleh, M. and Aliyari Shoorehdeli, M. “Multi-objective optimization of 6-degree-of-freedom cable-driven parallel robot using kinematic indices.” *Journal of Control*, Vol. 7, No. 2, pp. 43–56, 2013.
 6. Zi, B., Zhu, Z.c. and Du, J.I. “Analysis and control of the cable-supporting system including actuator dynamics.” *Control Engineering Practice*, Vol. 19, No. 5, pp. 491–501, 2011.
 7. Khalilpour, S.A., Loloie, A.Z., Taghirad, H.D. and Masouleh, M.T. “Feasible kinematic sensitivity in cable robots based on interval analysis.” In “Cable-Driven Parallel Robots,” pp. 233–249. Springer, 2013.
 8. Miermeister, P., Pott, A. and Verl, A. “Auto-calibration method for overconstrained cable-driven parallel robots.” In “ROBOTIK 2012; 7th German Conference on Robotics,” pp. 1–6. VDE, 2012.
 9. Hosseini, M.I., Harandi, M.J., Khalilpour, S.A. and Taghirad, H.D. “Adaptive fast terminal sliding mode control of a suspended cable-driven robot.” In “2019 27th Iranian Conference on Electrical Engineering (ICEE),” pp. 985–990. IEEE, 2019.
 10. Lessanibahri, S., Cardou, P. and Caro, S. “A cable-driven parallel robot with an embedded tilt-roll wrist.” *Journal of Mechanisms and Robotics*, Vol. 12, No. 2, 2020.
 11. Mottola, G., Gosselin, C. and Carricato, M. “Dynamically feasible motions of a class of purely-translational cable-suspended parallel robots.” *Mechanism and Machine Theory*, Vol. 132, pp. 193–206, 2019.
 12. Filipovic, M., Djuric, A. and Kevac, L. “Influence of the construction type of a cable-suspended parallel robot on its kinematic and dynamic model.” *Scientific-Technical Review, Military Technical Institute, Belgrade, Serbia, ISSN*, Vol. 206, p. 2013, 1820.
 13. Riehl, N., Gouttefarde, M., Krut, S., Baradat, C. and Pierrot, F. “Effects of non-negligible cable mass on the static behavior of large workspace cable-driven parallel mechanisms.” In “2009 IEEE international conference on robotics and automation,” pp. 2193–2198. IEEE, 2009.
 14. Taghirad, H.D. *Parallel robots: mechanics and control*. CRC press, 2013.
 15. Lessanibahri, S., Cardou, P. and Caro, S. “Kinetostatic analysis of a simple cable-driven parallel crane.” In “International Design Engineering Technical Conferences and Computers and Information in Engineering Conference,” Vol. 51807, p. V05AT07A049. American Society of Mechanical Engineers, 2018.
 16. Salisbury, J.K. and Craig, J.J. “Articulated hands: Force control and kinematic issues.” *The International journal of Robotics research*, Vol. 1, No. 1, pp. 4–17, 1982.
 17. Gosselin, C. and Angeles, J. “A global performance index for the kinematic optimization of robotic manipulators,” 1991.
 18. Behzadipour, S. and Khajepour, A. “Stiffness of cable-based parallel manipulators with application to stability analysis,” 2006.
 19. Abdolshah, S., Zanotto, D., Rosati, G. and Agrawal, S.K. “Optimizing stiffness and dexterity of planar adaptive cable-driven parallel robots.” *Journal of Mechanisms and Robotics*, Vol. 9, No. 3, 2017.
 20. Yeo, S., Yang, G. and Lim, W. “Design and analysis of cable-driven manipulators with variable stiffness.” *Mechanism and Machine Theory*, Vol. 69, pp. 230–244, 2013.
 21. Loloie, A.Z. and Taghirad, H.D. “Controllable workspace of cable-driven redundant parallel manipulators by fundamental wrench analysis.” *Transactions of the Canadian Society for Mechanical Engineering*, Vol. 36, No. 3, pp. 297–314, 2012.